JOURNAL OF MATERIALS SCIENCE 9 (1974) 809–820

On the phenomenon of grain-boundary hardening in iron

M. BRAUNOVIC
IREQ, Hydro-Quebec Institute of Research, Varennes, Quebec, Canada

C. W. HAWORTH
Department of Metallurgy, University of Sheffield, UK

Microhardness measurements on a fully recrystallized Fe-0.02 at. % W alloy show the existence of a region extending some 40 μm on either side of the grain boundaries, where the hardness is up to 35% higher than that of the grain. The magnitude of the hardening is partly controlled by the effective resolution of the hardness test because of the steeply increasing hardness near the boundaries. In addition, for small grain sizes, overlapping hardening profiles from the boundaries may affect the grain-interior hardness. The position of the boundary, with respect to the metallographic surface, significantly affects the width of the hardening; this width is increased on that side of the boundary where its inclination with respect to the surface of the specimen is increased. The results show that the excess, hardening at the boundary is a real hardening effect comparable to other hardening effects and that we should expect a marked inhomogeneity of bulk mechanical properties even for a relatively pure alloy.

1. Introduction

The variation in hardness across a grain boundary, observed from a sequence of microhardness impressions, is a well documented effect. It has been shown [1] that for very pure lead and zinc there is an apparent softening at the boundaries but that very small additions of certain alloying elements change this to an apparent hardening. For iron there are no published data showing zero hardening or grain-boundary softening, but there is evidence for an increasing grain-boundary hardening effect with increasing impurity content [2] although deliberate addition of W or Mo [3] or C [4] is known to eliminate the effect. Whilst the cause of the hardening is not known, it is believed to be associated with the migration of some species (possibly vacancies or vacancy-solute complexes) to the boundary during the annealing treatment or during the cooling from the final heat-treatment.

One aspect of the phenomenon which is cause for some concern is whether the measured grain-boundary hardening is a property of the grain boundaries throughout the bulk of the material and can be understood on the same basis as "normal" hardness, or whether it is really a property of the metallographic surface of the specimen introduced into the surface (near the grain boundaries) during the metallographic preparation or, perhaps, an intrinsic surface contribution to the microhardness measurement which differs from the grain interior to the vicinity of the grain boundary.

If the observed grain-boundary hardening can be interpreted as a "surface" effect, then whilst it still has interest and could be of significance, it would not necessarily have the same significance for the bulk mechanical and other properties of the material. On the other hand, if the increased hardness at the grain boundaries, which can be as much as 35% of the grain hardness, is a property of the boundaries throughout the bulk of the specimen, then such inhomogeneity in the specimen would be expected to be an important feature in any deformation studies. Inasmuch as micro-indentation hardness testing is by far the most successful technique used in detecting the anomalies occurring in the boundary affected regions, it will be advantageous to summarize some definitions, formulae and experimental facts concerning the micro-indentation hardness testing. From these general principles, the particular applications to the

problems studied in the present work can be envisaged.

2. Basic features of micro-indentation hardness testing

Indentation hardness can be defined as the resistance of a specimen to the penetration of a non-deformable indenter under the action of a force. It is generally expressed as the ratio of the applied force or load (P) to the total surface area (A) of the impression. The area of the impression can be calculated for the various shapes of the indenting diamond from a characteristic length measured under the microscope. Hardness is thus generally given by

$$H = K(P/A)\ \mathrm{kg\ mm^{-2}} \qquad (1)$$

where K is a constant depending upon the shape and the type of the indenter. Hence, the Vickers hardness (tetragonal pyramid) corresponding to an impression of diameter (diagonal) d, is given as

$$H = 1854.4\,(P/d^2)\ \mathrm{kg\ mm^{-2}} \qquad (2)$$

where P is expressed in grams and d in microns.

One of the most controversial aspects of indentation hardness testing at low loads is the dependence of hardness on load, which is usually found by considering the relationship between the load, P, and the diameter (diagonal), d, of the impression. In order to describe this load dependence, several different relationships between load and diagonal have been proposed. One well known and frequently applied relation is an empirical rule expressing the load dependence upon diagonal as:

$$P = a\,d^n\,. \qquad (3)$$

This equation has become established in the literature as the "Meyer formula", and the exponent n is known as the "Meyer index". By combining Equations 2 and 3 one can obtain

$$H = a_1 d^{(n-2)}\,. \qquad (4)$$

It is essential, however, to emphasize that numerous measurements have established that this formula is never strictly valid. The rational use of the exponent n (the "logarithmic index") is, therefore, confined to comparative studies made within limited ranges of measurements, thereby ensuring that Equation 3 is approximately satisfied. One can then attempt to interpret the variation of the mean value of n, which is used as an empirical parameter of complex significance.

For experimental data obtained under strictly controlled conditions of measurements, there are two alternative methods of representing these results. One is by plotting the curves of log $P = f(\log d)$; the second is to plot curves of $H = f(\log P)$. The problem, then, lies only in the correct interpretation of the various shapes of the curves representing the measured data.

According to Bückle [5] when measurements are carried out in the absence of all possible causes of error on metals or phases that are pure, homogeneous and have undisturbed monocrystalline or very coarse-grained structures, the results invariably give curves of the shapes illustrated in Fig. 1. These curves can be regarded as the "basic form" of Vickers hardness curves. The curve shown in Fig. 1a lies between two asymptotes of slope $n = 2$, which appear in the hardness-load diagram as horizontal asymptotes. In other words, the hardness tends to assume constant values not only for increasing loads but also for decreasing loads, a fact which is not evident *a priori*.

When the specimen is heterogeneous or otherwise disturbed, the curves often take the form illustrated in Fig. 1b. There is always a tendency for the curves to take on the "basic form" represented in Fig. 1a. However, this basic form is obtained only with very large indentations (loads), or where the indentations are small enough to reflect the behaviour of the pure matrix. With medium sized indentations (medium loads), as a result of the influence of the structural factors, the basic form of the curves will be distorted.

The influence of the microstructure on the load dependence and, in general, on the hardness can be explained by the mechanism of penetration of the indenter into the material. The basic elements of the penetration mechanism are mobile dislocations and their mean free path. The generation of dislocations at a contact interface can be visualized as arising from a punching mechanism. When an indenter is strongly pressed against the surface of a metal it creates an impression by introducing loops of dislocations. As the dislocation loops expand from the source their movement may effectively be impeded by pinning and blocking by lattice defects such as grain boundaries, vacancies, solute atoms, precipitates, and similar imperfections. This is shown schematically in Fig. 2,

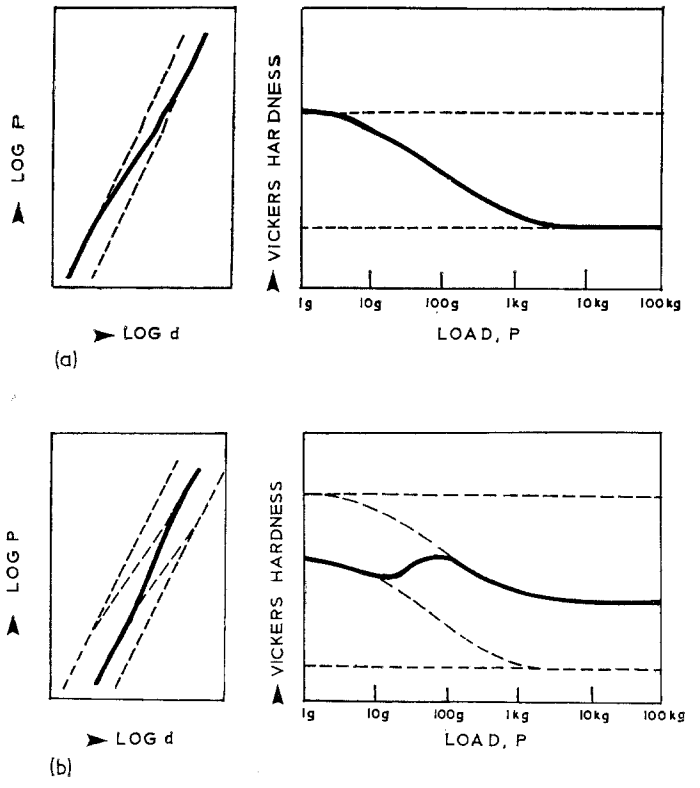

Figure 1 General forms of hardness-diagonal (log P/log d) and hardness load (H/P) curves for (a) undisturbed single crystal, (b) heterogeneous specimen.

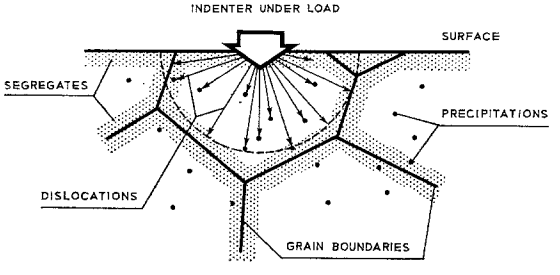

Figure 2 Schematic representation of the penetration mechanism characterizing the micro-indentation.

where the dislocations generated by the indenter are blocked by the obstacles. Obviously, the true mechanism is much more complex, but this rather simplified model can, nevertheless, adequately describe the effects of various lattice imperfections on the indentation hardness.

The stress required to move dislocations is a measure of the flow stress of the material sampled by the indenter. According to Tabor [6], at a "representative strain" (generally considered to be 8%) characteristic of the indenter, the hardness, H, of a metal is related to the flow stress, σ, as

$$H = c\sigma \tag{5}$$

where c is a proportionality constant that takes different values depending on the type of the indenter and tester used, but generally lies [7] in the range 3 to 6.

One interesting feature of the curves shown in Fig. 1 is the overall apparent increase in hardness with decreasing load. The phenomenon appears to be genuine and in no way associated with the instrumental errors or the preparative treatment of the surface. There have been several explanations offered for the observed phenomenon and reference is made here to the recent work of Gane and Cox [8] where these explanations are discussed in detail. Another feature of micro-indentation hardness testing that is cause for concern is the elastic recovery that the impression undergoes after the indenter is withdrawn from the material. This feature has recently been investigated by Braunovic and Haworth [9] who have shown that the elastic recovery that the

indentation undergoes, following removal of the indenter, is found to take place almost entirely in the direction of the depth whereas the contraction of the diagonals is practically negligible.

3. Materials and specimen preparation

In the present study, the alloy used was iron containing $\sim$ 200 at. ppm of tungsten. This alloy is one of the series of Fe-W alloys used for the study of the effects of alloying additions on the grain-boundary hardening [2], and is the alloy which shows a maximum boundary hardening effect ($>$ 35% increase in hardness for a load of 3.3 g). The "pure" base iron showed a somewhat smaller hardening effect.

The alloy was prepared by remelting a master alloy (containing 3 at.% W) with Glidden electrolytic iron flakes in a non-consumable tungsten electrode argon-arc furnace. Repeated melting was used to improve the homogeneity of the button. Analysis gave: $O_2 \sim 100$; C $\sim$ 40; $N_2 \sim 20$; and substitutional impurities $\sim$ 200 at. ppm. Details of the alloy preparation and a full analysis are given elsewhere [2]. The ingot was then swaged to an 8 mm diameter bar, chemically polished and given a heat-treatment in a vacuum of 10^{-5} Torr for 2 h at 1450°C to remove short-range segregation. A subsequent grain-refinement treatment was given by quenching into water after annealing for 2 h at 1100°C in an evacuated silica capsule, before swaging to the final diameter of 5 mm.

Before all heat-treatments the specimens (1 cm long) were chemically polished in 3 parts H_3PO_4 + 2 parts H_2O_2 (100 vol) for 10 min, washed with alcohol, carefully dried, and sealed under 10^{-5} Torr vacuum in silica capsules. Specimens were recrystallized at 800°C for 2 h, cooled to 700°C, held for 24 h and furnace-cooled at a rate of $\sim$ 50°C h^{-1}.

4. Microhardness measurements

Specimens for microhardness testing were first ground on wet silicon carbide papers and polished on 6 and 0.25 μm diamond paste. To obtain reliable microhardness data, it was necessary to remove the strained surface layer [10] by electropolishing. The electropolishing solution was 700 ml methanol with 100 ml each of perchloric acid, glycerine and water. The grain boundaries were revealed by slightly changing the electropolishing conditions. The electropolishing procedure was repeated until a constant value for the grain hardness was obtained. Since it was thought that the metallographic preparation may have been responsible for the hardening effect, different techniques for surface preparation were employed, but in all cases a grain-boundary hardening was observed. Electropolishing was the simplest and most reliable procedure.

The measurements were carried out on a Reichert microhardness tester, in which the indenter was loaded by a manually operated spring mechanism. Except where otherwise stated the applied load was 3.3 g, giving an indentation diagonal of 7 to 8.5 μm. The error in the hardness values was mainly associated with measuring the diagonal, and corresponded to a relative error in hardness for one indentation of about 5% at the 95% confidence level. An indentation could be positioned on the specimen to a precision of location of about 0.5 μm and, subsequently, distances from a grain boundary or other reference surface to the centre of a particular impression of the order of 10 to 100 μm could be measured with the same precision.

4.1. Hardness measurements and the sub-surface distribution of grain boundaries

In these experiments, hardness measurements were obtained for that part of the specimen for which the detailed three-dimensional grain-boundary topology was also known. This part of the specimen is shown in Fig. 3. Several sections were used, the sections being removed by electropolishing, the thickness of the section being measured by careful weighing of the specimen, and the relative positions of consecutive sections being located by large pyramidal indentations placed in a neighbouring part of the specimen. These indentations were never entirely removed by the electropolishing. The dotted lines in Fig. 3 show the position of the boundaries about 12 μm below the surface on which the microhardness values are obtained. This position was used to determine the angles (θ) between the sub-surface boundaries and the free surface of the grain on which the test is made.

The results of hardness measurements are shown in Fig. 4 as hardness-distance profiles for different grain boundaries that have been traversed as shown in Fig. 3. When the impression is located in the centre of a large grain where grain boundaries are not involved, the apparent

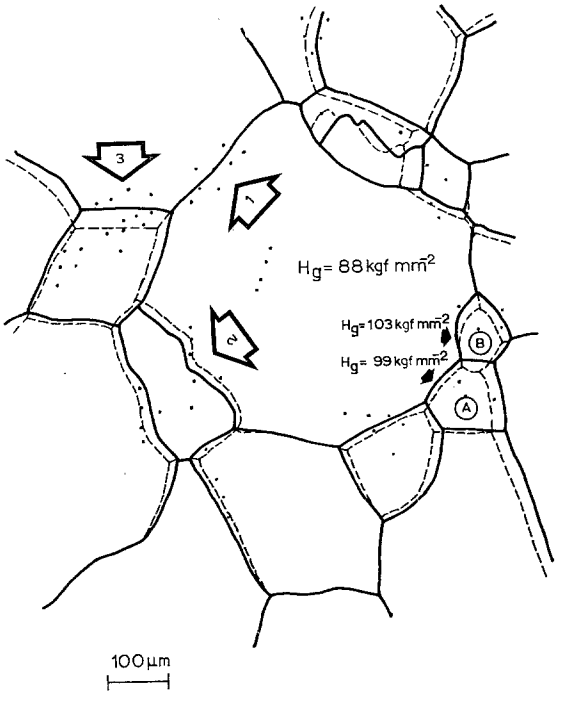

Figure 3 Microhardness impressions (load 3.3 g) located relative to grain boundaries (full lines). Broken lines indicate relative positions of boundaries 12 μm below the surface of the specimen.

hardness of the grain interior is 88 kg mm^{-2}. On the other hand, for the impressions located in the centres of the two small grains marked A and B in Fig. 3, of apparent dimensions of $\sim$ 100 μm (or more), the hardness values are 99 and 103 kg mm^{-2}, i.e. above the normal grain interior hardness value of 88 kg mm^{-2}. These values can be understood by reference to Fig. 4, showing the effect of inclination angle θ on the shape of the hardness-distance profile across different boundaries. When the boundary is perpendicular to the free surface of the specimen on which microhardness measurements are carried out (θ = 90°), the hardness-distance profile is symmetrical with respect to the boundary (Fig. 4a). The hardening is just detected with an impression located at $\sim$ 30 μm either side of the boundary. Such dependence is observed at the grain boundary marked 1 in Fig. 3.

However, when the boundary is inclined to the free surface, as in the cases of the grain boundaries marked 2 and 3 in Fig. 3, the hardness-distance profiles are asymmetrical, i.e. higher hardness values are obtained for impressions located at distances somewhat greater than 40 μm

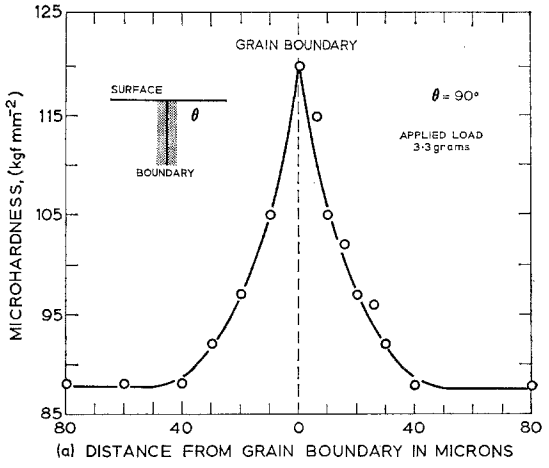

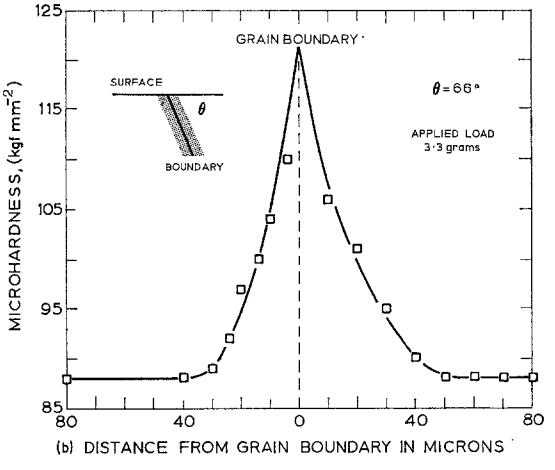

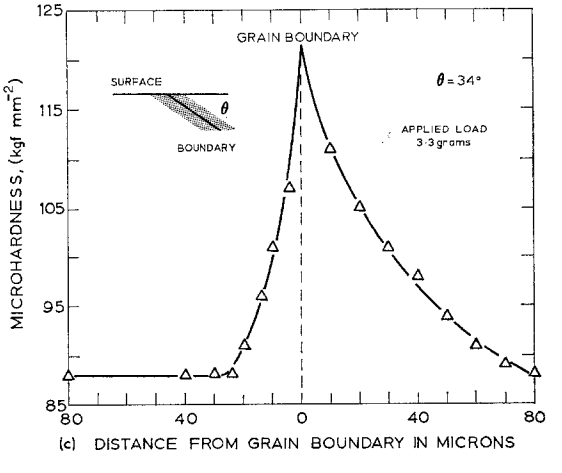

Figure 4 (a) to (c) Boundary profiles for different values of θ (angle between boundary and metallographic surface)

on the side of the boundary for which $\theta < 90°$. The implication is that these higher hardness values are due to the fact that the impressions are detecting hardening associated with the sub-surface boundaries. In other words, these results established that a real hardening is present in the neighbourhood of the grain boundary, of much the same shape as the observed (symmetrical) profile (Fig. 4a), extending up to 40 μm either side of the boundary, and is coupled with an averaging based on the resolution of the hardness test to produce the apparent hardening. This is clearly illustrated in Fig. 5 where the data for several profiles are shown as a function of *perpendicular* distance between the location of the test and the boundary. It is apparent that the data tend to a common set corresponding to $\theta = 90°$. Thus the anomalously high hardness values from the impressions located in the centres of the two small grains A and B (more than 40 μm from the nearest boundary) are obtained by picking up the hardening associated with the sub-surface boundaries, since the indenter is penetrating *towards* the hardened boundaries. On the other hand, the lower hardness values obtained for the impressions located at distances somewhat smaller than 40 μm on the side of the boundary for which $\theta > 90°$ (Fig. 4b and c) can be explained in terms of sampling the softer material by the indentation, since the indenter penetrates towards the softer grain interior.

It is interesting to note that Arkharov *et al* [11] observed a similar effect of boundaries on hardness. They found that the hardness measured on the concave side was higher than that on the convex side of the boundary.

4.2. Apparent extent and magnitude of grain-boundary hardening

It has already been shown that for slowly cooled specimens the hardening appears to extend to some 40 μm either side of the boundary for measurements made with a load of 3.3 g on the indenter. Fig. 6 shows the effect of using different loads on the indenter; as the load is increased the apparent width of the hardened region does not increase, although the apparent magnitude of the hardening at the boundary, and at any given position relative to the boundary, decreases with increasing load on the indenter.

Using the larger loads on the indenter will increase the volume that is tested and thus change the effective resolution of the technique. It is this decrease in resolution with increasing load that is believed to be responsible for the change in peak hardness with load shown in Fig. 6. Consequently, the smaller the load, the smaller will be the difference between apparent and true hardness values. On the other hand, the constancy of the width of the hardened region for different loads used shows that in this case the change in the resolution of the technique for the range of loads used does not affect the extent of the apparent hardening (40 μm on either side of the boundary) and, hence, this is believed to be the extent of the true hardening.

The width of the hardened region was deter-

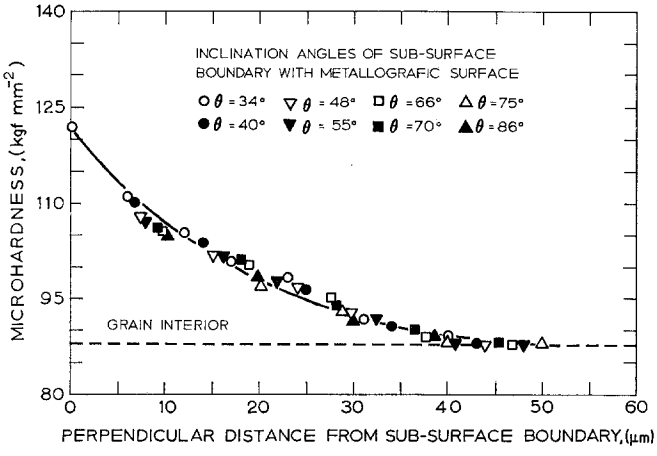

Figure 5 Hardness as a function of perpendicular distance to plane of boundary.

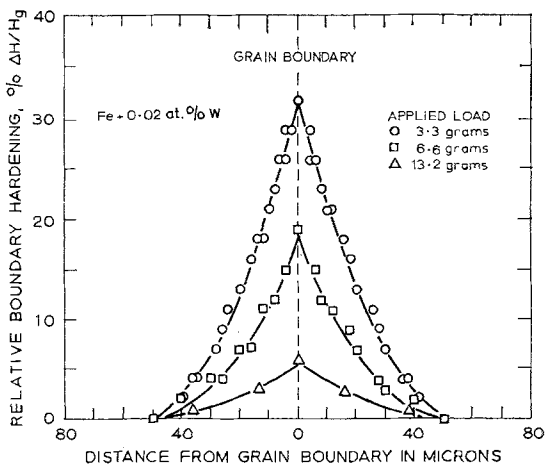

Figure 6 Hardness profiles across a boundary normal to the metallographic surface ($\theta = 90°$) for a range of applied loads.

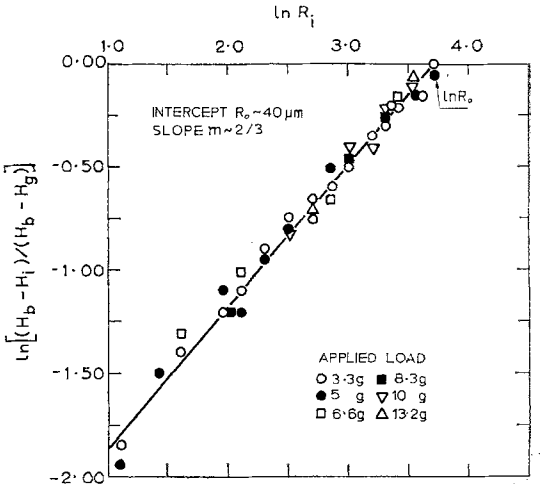

Figure 7 The log/log plot of hardness profile data according to Equation 6.

mined more rigorously using an empirical formula for the hardness increment-distance dependence, given as

$$\Delta H_i = \Delta H_b \left[1 - (R_i/R_0)^n\right] \qquad (6)$$

where $\Delta H_i = H_i - H_0$ and $\Delta H_b = H_b - H_0$; H_i, H_0, and H_b are hardness values measured at distance R_i from the boundary, in the bulk of the grain for which $R_i = \infty$, and at the boundary, respectively. R_0 is the distance where $H_i = H_0$, or the extent of the apparent hardening.

By plotting the data from Fig. 6 in the form of

$$\ln (1 - \Delta H_i/\Delta H_b) = f(\ln R_i)$$

as shown in Fig. 7, R_0 and exponent n can be evaluated as an intercept and a slope, respectively. As seen from this figure, data for all the loads used fall on the same line; the slope and that intercept of this line for which $\ln (1 - \Delta H_i/\Delta H_b) = 0$ where calculated by the least-squares analysis, giving the following values: $n = 0.66 \simeq 2/3$ and $R_0 \simeq 40$ μm. It must be emphasized, however, that this simple relationship is purely empirical, and the true hardness-distance dependence is believed to be more complex, requiring a detailed knowledge of the processes occurring in the vicinity of a grain boundary.

On the other hand, the constancy of the value of the exponent $n = 2/3$ that is found when Equation 1 is applied to all the hardness-distance data, implies that Equation 1 expresses as:

$$\frac{H_b - H_i}{H_b - H_0} = \left(\frac{R_i}{R_0}\right)^{2/3} \qquad (7)$$

may well be used as to describe adequately the observed hardness-distance dependence of the boundary hardening and thus for a more rigorous determination of the apparent extent of boundary hardening, i.e. R_0.

4.3. Grain-size effect

The presence or absence, and in particular the magnitude, of grain-boundary hardening will depend upon grain size if there is any overlapping of the hardening profile in the centre of the grains. To study this effect, a range of grain sizes was produced by further swaging to give 1.7 mm diameter wires of the same alloy as used previously, and then annealing at temperature in the range 650 to 890° C for times of 10 min to 24 h. The specimens were either furnace-cooled or slowly air-cooled. From the results there appeared to be no significant difference between these two cooling rates as far as the boundary-hardening effects were concerned. In all cases care was taken to check that the structures were fully recrystallized with no sub-structure. Grain sizes were measured on longitudinal metallographic sections using the circular intercept method and measuring approximately 500 intersections.

The microhardness measurements were made with 3.3, 5, 8 and 13.2 g loads, the procedure being to measure points randomly selected at

various grains and grain boundaries. Each reported measurement is the average of ten indentations. The grain-boundary indentations were located at the grain boundaries and away from three-grain junctions, whereas the grain-interior indentations were taken from the centres of the grains. The results of the microhardness measurements are shown in Figs. 8 and 9. In Fig. 8, hardness data for loads of 3.3 and 5 g are presented as an illustration, since similar behaviour was observed for 8 and 13.2 g loads. The complete data from microhardness measurements for all loads used are shown in Fig. 9, as the grain-boundary hardness increment ($\Delta H/H_g$) versus average grain size.

From Fig. 8, it is clear that the hardness of the grain boundaries remains independent of the change in the grain size, whereas the hardness of the grain interiors decreases as the grain size increases. For some "critical" grain size. apparently different for different loads, the hardness of the grain interior levels off and remains constant with further increase in grain size. Consequently, the grain-boundary hardness increment ($\Delta H/H_g$) will initially increase with increasing grain size, but will attain a constant value (different for different loads) after the "critical" grain size is passed. This is illustrated in Fig. 9. Although the data are not sufficiently good for precise values to be obtained, reasonable distinction can be made between the "critical" grain sizes for different loads, and values of about 85, 95, 100 and 120 μm can be ascribed for loads of 3.3, 5, 8 and 13.2 g respectively. The

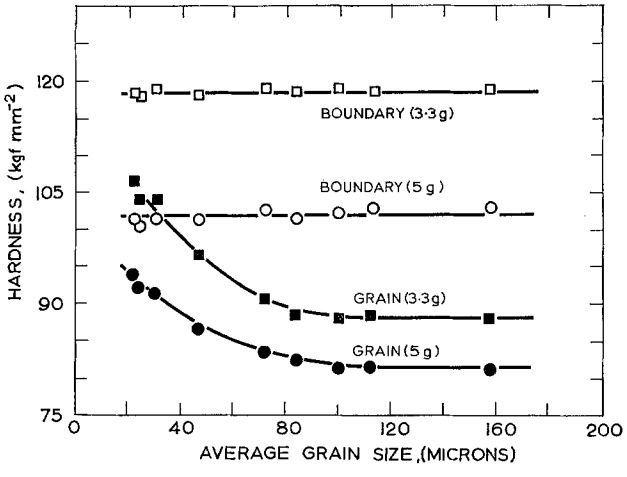

Figure 8 Variation of microhardness with grain size.

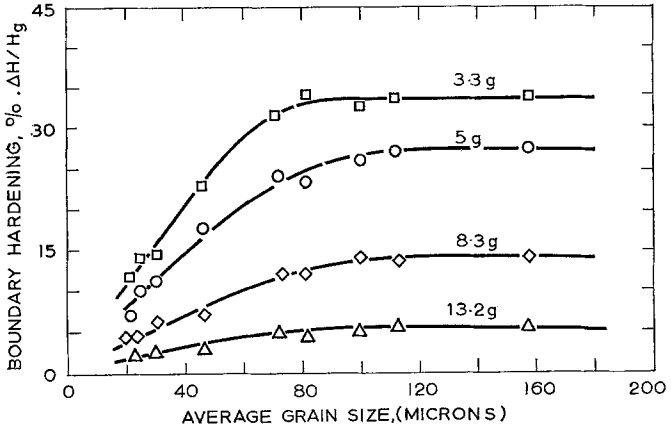

Figure 9 Relative hardness increment, $\Delta H_b = (H_b - H_g)/H_g$, as a function of grain size for different loads used.

fact that these "critical" grain sizes increase with increasing load on the indenter, suggests that the hardening found to extend 40 μm either side of the boundary is detected by the loads used when their zone of influence begins to "feel" the presence of this hardening at the grain boundaries. Hence, the measured grain-interior hardness values for grains with sizes smaller than these "critical" ones, reflect the grain-boundary hardness-distance dependence for the loads used and, as a result of this, the hardness of the grain interiors is raised. A similar effect was observed by Bückle [5] in electrolytic iron.

A fuller understanding of the microhardness test and the detection of grain-boundary hardening can be obtained from Fig. 10. Microhardness data for two specimens of iron + 200 at. ppm

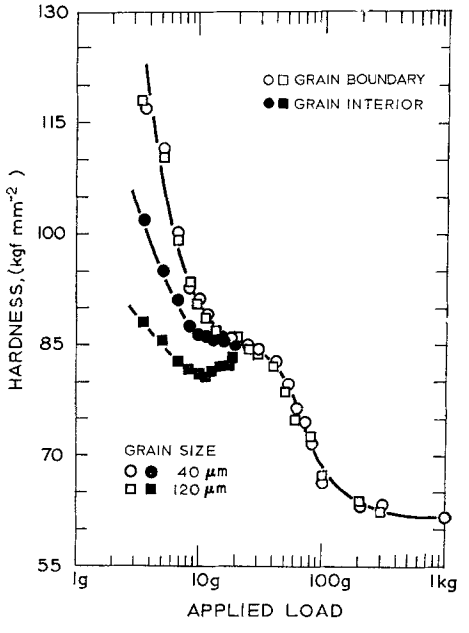

Figure 10 Variation of hardness with load for grain interior and grain boundaries using specimens of two different grain sizes.

tungsten with grain sizes of 40 and 120 μm were obtained using a range of loads from ~ 3 g to 1 kg. Indentations were located in the centres of the grains and at randomly selected grain boundaries. Each reported value is an average of ten readings.

The general feature of the data shown is that for loads up to about 30 g there are three basic curves whilst at loads greater than 30 g all the data are represented by one curve. The basic curve representing the grain-boundary hardness data shows the highest hardness values. Similar behaviour, but with lower hardness values, is shown by the curve representing the grain-interior hardness data of the specimen with the fine grain (40 μm). The curve with the lowest hardness values shows the grain-interior hardness data of the specimen with a grain size of ~ 120 μm. The presence of the displacement ("kink") in the latter hardness-load curve is quite obvious from Fig. 9, and is associated with the effect of grain boundaries. The effect can be explained in terms of the zone of influence around the impression, in conjunction with the hardening effect that occurs in the regions close to the grain boundaries. In other words, application of low loads up to a certain limit will yield practically single-crystal hardness values, as long as the zone of influence of the impression is so small as to not detect the regions near the grain boundaries where hardening occurs. The results in this load range can be represented by a section of the basic curve, as shown in Fig. 1a, that applies to a homogeneous structure.

With further increasing load, the zone of influence will exceed the grain size and polycrystalline testing conditions will be reached where the specimen behaves in a quasi-homogeneous manner. As pointed out in Section 2, the results obtained in the latter load range can also be represented by a basic curve which will obviously give higher hardness values than a single crystal basic curve (Fig. 1b). Hence, the presence of the displacement ("kink") in the hardness-load curve indicates a transition from one basic curve to another due to the fact that the zone of influence of the impression for the load range where the displacement occurs approaches the grain size. It is interesting to note that the zone of influence of the impression is found to be ~ 10 times the depth of the indenter penetration [9].

In view of the foregoing remarks, the hardness data for the fine (40 μm) and coarse (120 μm) grain sizes can be divided into two regions in order to simplify discussion.

(a) For loads < 30 g, whilst the boundary hardness is independent of grain size, the grain interior hardness is higher for the smaller grain sizes. This is because the extent of the hardening associated with the boundaries overlaps in the centre of the 40 μm grains. For the larger grain sizes the increase in grain hardness with increasing load (in the range 10 to 20 g)

comes about because the indentation samples the harder boundary "material" to an increasing extent as the load is increased.

(b) For loads > 30 g, the boundary and grain-interior hardnesses have the same value for a given load (for clarity the grain interior values are omitted from the graph). Under these conditions the indenter is averaging the polycrystalline hardness of the specimen.

5. Discussion

The detection of hardening from sub-surface boundaries, and the detailed understanding of microhardness data which has been demonstrated in Section 4, indicate that the grain-boundary hardening observed in iron is a well established phenomenon which may well be an important feature in the interpretation of bulk mechanical properties. Further confirmation that the boundary hardening is a measure of a property of grain boundaries throughout the crystal is provided by a grain-boundary contribution to electrical resistivity which has been found in the specimens used in the present work and is reported elsewhere [11]. This contribution is detectable at room temperature but is relatively large at low temperatures. It is significant that the observed variation of resistivity with grain size can be explained in terms of a grain-boundary layer, approximately 60 μm wide, of higher resistivity than the remainder of the grains.

Furthermore, most recently, Braunovic and Haworth [12] have shown that the elastic recovery behaviour of the micro-indentations located at grain boundaries is different from those located in the bulk of the material (grain interior). The amount of contraction in the direction of depth is load-dependent; in the low-load range (< 25 g), this contraction is larger for the bulk indentations than for those located at the grain boundaries. For loads above 25 g, there is no difference in the amount of contraction for bulk and boundary indentations. Disappearance of this divergence is consistent with grain-boundary hardening which diminishes as the load on the indenter is increased (see Fig. 6). Such good correlation between these two effects implies that they are not due to the intrinsic nature of the microhardness testing but are rather a measure of a property of grain boundaries throughout the crystal.

It should be emphasized, however, that owing to the complex nature of the deformation of a material caused by pyramid indentation, the real nature of grain-boundary hardening is rather difficult to envisage. The reasons for such uncertainty appear to be as follows. If one speaks in terms of micro-indentations performed by applying to the indenter very small forces (loads below some critical level), then the hardness excess detected at the grain boundaries exhibits all the characteristic features of a real hardening process such as surface hardening (case-hardening, mechanical and thermal treatments of surfaces). On the other hand, when higher loads (above critical level) are applied, this effect loses its significance and, at first sight, it would appear as if this is not a real hardening phenomenon. This is because when higher loads are applied on the indenter, the micro-indentation hardness testing loses its sensitivity and owing to the lack of resolution the effect would not be revealed.

A similar effect has also been observed in the case of surface hardening following various mechanical finishes of pure iron [10]. It has been shown that the lack of resolution associated with higher loads masked the work-hardening effect at the metal surfaces otherwise revealed by the use of smaller loads. The results described in Section 4.3 provide further support. It was shown that the general shape of the hardness-load curve is determined by the properties of the material. Since it is generally accepted that this curve expresses the hardness behaviour of material [5], it seems fairly obvious that the observed hardening at grain boundaries should be considered in these terms. Hence, any deviation from the basic form has to be considered as an anomaly which, in the absence of experimental errors, should be explicable in terms of microstructure. Since the hardening occurring at a grain boundary causes the same distortion of the hardness curves as, say, surface hardening of a material [5, 10], it is clear that this is a real hardening phenomenon. In other words, material in the boundary is indeed *hard* in the real meaning of the word.

It is of interest to note that the distortion of the hardness curves was used by Braunovic and Haworth [10] to determine the thickness of the surface-hardened layers following various mechanical finishes of pure iron. The presence of such internal heterogeneities (or property gradients) in a material should have a significant influence on its bulk mechanical properties. Consequently, it is obvious that plastic flow of a

material will be strongly affected by grain-boundary hardening. Such an effect will be most strongly reflected through the Hall-Petch relationship between the yield or flow stress, σ, and the grain size, L, that is:

$$\sigma = \sigma_0 + kL^{-\frac{1}{2}} \quad (8)$$

where σ_0 and k are constants. Unfortunately, so far little has been done in this respect to provide more direct and definite evidence for such an effect. Some attempts, nevertheless, have been made to establish a correlation between the constants σ_0 and k and grain-boundary hardening. Karavaeva and Sukhovarov [13] have found that an intensive segregation of impurities at grain boundaries strongly affects the parameters σ_0 and k and also is a cause for considerable grain-boundary hardening in pure Ni. It is shown that there is a correlation between the variation in the parameters σ_0 and k and the change in grain-boundary hardening: the sharp decrease in k and increase in σ_0 corresponded well with the rapid decrease in grain-boundary hardening following quenching from above a certain critical temperature ($> 600°C$). They concluded that the observed changes in σ_0 and k and grain-boundary hardening are due to changes in impurity segregation to the grain boundaries caused by the different thermal treatments.

Shashkov [14] has shown that with increase in the grain size of polycrystalline intermetallic compounds, the brittle-to-ductile transition temperature falls in exactly the same way as does the grain-boundary hardness; the lower the grain-boundary hardness, the lower is the brittle-to-ductile transition point of the compound and vice versa. It is noteworthy that Shashkov has found an opposite dependence of grain-boundary and grain-interior hardness on the grain size as compared with the results of this study (Fig. 8). According to his results, it is the grain-boundary hardness that increases with increasing grain size, whilst the grain-interior hardness remains constant.

It should be pointed out, however, that an *ad hoc* explanation for such a difference in the grain-size dependence of grain-boundary hardening is rather difficult to envisage as in Shashkov's work neither the experimental details concerning the microhardness measurements nor the actual heat-treatments used for producing different grain sizes are well defined. On the other hand, it might be speculated that the loads used by Shashkov were small enough to allow the intrinsic behaviour of both grain boundary and grain interior to be measured*. Another possibility is that heat-treatments used for the production of different grain sizes might be responsible for the observed increase of grain-boundary hardness. In other words, if higher temperatures were used to produce larger grain sizes, then the observed variation of the grain-boundary hardness may well be the result of quenching, that is, temperature, rather than of the grain size change. Further support that this may indeed be the case comes from the same work of Shashkov, showing that the hardness of the grain boundaries rises exponentially with quenching temperature. In the present work, however, different grain sizes were produced by slow cooling from different temperatures, which eliminated the effect of quenching.

More recently, Floreen and Westbrook [15] have shown that in nickel, the grain-boundary hardening and the parameter k are affected not only by the heat-treatment but also by the amount of solute segregated at the grain boundaries. They have shown that with progressive additions of sulphur to nickel, the grain boundary hardening increases whilst at the same time a very unusual variation in k occurs. It is found that k initially increases with sulphur additions, reaches a maximum value and, with further additions of sulphur, steadily decreases. No definite and conclusive explanations were given, but it was suggested that such a variation in k cannot be readily explained in terms of the dislocation pile-up mechanism and that the grain-boundary ledge model of Li [16] apparently provides a much better basis for rationalizing the parameter k.

Somewhat similar results have been reported in iron by Braunovic and Haworth [17] who have shown that the slope of the hardness-grain size curve (H versus $L^{-\frac{1}{2}}$) increases with increasing impurity content. They rationalized such an effect in terms of Li's grain-boundary ledge model.

To summarize, the presence of the excess hardening extending to a considerable width on either side of the boundary indicates that processes occurring in such a wide region involve a greater part of the lattice than was previously supposed. The presence of such a wide region

*The authors are indebted to Dr J. H. Westbrook for this suggestion.

seems to be readily plausible since the experimental evidence indicates that various anomalies observed in the bulk properties and at the grain boundaries cannot be sufficiently and adequately explained in terms of a transition lattice of the order of 2 to 3 atomic distances in width. This, however, in no way implies that there is no such transition zone on an atomic scale where two perfect lattices meet each other, since its presence has been abundantly confirmed. In fact, the main point of the concept of a wide, boundary-affected region is based *not* on the actual width of the boundary, but on the processes occurring within such a perturbed zone of a lattice. The nature of the perturbation involved is obviously complex and presumably involves different interaction mechanisms and processes, which may extend for a number of microns rather than atomic distances.

Finally, a word of caution should be added in that one should not universally apply the concept of a wide perturbed region in explaining the anomalies observed in the properties associated with grain boundaries, since there are still properties significantly affected by the grain boundaries for which the concept of a "thin" boundary may well provide better explanation, for instance, grain-boundary migration. It is, therefore, quite obvious that these two concepts are closely interrelated and exclusion of either of them cannot be justified.

6. Conclusions

The following conclusions can be drawn for the phenomena observed in this study.

1. The micro-indentation testing is a suitable probe for revealing local changes in hardness.

2. Excess hardening at the boundary is established as a real hardening effect.

3. The magnitude of boundary hardening is strongly dependent on load, whilst the width to which the hardening extends on either side of the boundary remains constant, irrespective of the load used. Boundary hardening in the tungsten-doped iron studied here could not be detected by loads greater than 20 g. In well annealed and furnace-cooled specimens this width is about 40 μm on either side of the boundary.

4. The position of the boundary, with respect to the metallographic surface, significantly affects the apparent width of the hardening. This width is increased on that side of the boundary where its inclination in respect to the surface of the specimen is increased.

5. Grain size affects the hardness of the grain interior rather than that of the boundary, which remains constant. An increase in the grain-interior hardness comes about because the extent of the hardening associated with the boundaries overlaps in the centre of the grain.

Acknowledgements

The authors are indebted to Professor A. G. Quarrell of Department of Metallurgy, University of Sheffield, for the provision of laboratory facilities where part of this work has been carried out. The authors are also thankful to Dr J. H. Westbrook of General Electric Co, Schenectady, for his interest and helpful discussions. Thanks are extended to Dr Edna A. Dancy of IREQ who read the final manuscript and made valuable comments.

References

1. K. T. AUST, R. E. HANEMANN, P. NIESSEN and J. H. WESTBROOK, *Acta Metallurgica* **16** (1968) 291.
2. M. BRAUNOVIC and C. W. HAWORTH, *Met. Sci. J.* **4** (1970) 85.
3. M. BRAUNOVIC, C. W. HAWORTH and R. T. WEINER, *ibid* **2** (1968) 67.
4. J. H. WESTBROOK and D. L. WOOD, unpublished work cited by J. R. LOW in "Progress in Materials Science", Vol. 12 (Pergamon Press, Oxford, 1963) p. 24.
5. H. BÜCKLE, *Met. Rev. London* **4** 13 (1959) 49.
6. D. TABOR, "The Hardness of Metals" (Clarendon Press, Oxford, 1951).
7. V. V. P. KUTUMBARAO and P. RAMA RAO, *Current Sci.* (India) **41** (1972) 523.
8. N. GANE and J. M. COX, *Phil. Mag.* **22** (1970) 881.
9. M. BRAUNOVIC and C. W. HAWORTH, *J. Mater. Sci.* **7** (1972) 763.
10. *Idem, Prakt. Metallog.* **7** (4) (1970) 183.
11. V. I. ARKHAROV, S. D. VANGENGEYM, S. K. KRYSOVA and V.Kh. PLASTOVETS, *Fiz. Metal. Metalloved.* **28** (1969) 304.
12. M. BRAUNOVIC and C. W. HAWORTH, *J. Appl. Phys.* **40** (1969) 3459.
13. V. V. KARAVAEVA and V. F. SUKHOVAROV, *Izvest. Vuz, Fizika*, **5** (1965) 40.
14. D. P. SHASHKOV, *Fiz. Metal. Metalloved.* **25** 3 (1968) 473.
15. S. FLOREEN and J. H. WESTBROOK, *Acta Metallurgica*, **17** (1969) 1175.
16. J. C. M. LI, *Trans. Met. Soc. AIME* **227** (1963) 239.
17. M. BRAUNOVIC and C. W. HAWORTH, 2nd International Conference on the Strength of Metals and Alloys, Asilomar (1970) Vol. I, p. 311.

Received 1 November and accepted 9 November 1973.